EXPERIMENTAL ANALYSIS OF DEHUMIDIFICATION HEAT TRANSFER CHARACTERISTICS ON COPPER SURFACES

by

Abhay Varghese Thomas

A Thesis Submitted to the Graduate

Faculty of Rensselaer Polytechnic Institute

in Partial Fulfillment of the

Requirements for the degree of

MASTER OF SCIENCE

Major Subject: MECHANICAL ENGINEERING

Approved by the
Examining Committee:

_____
Prof. Dr. Yoav Peles, Thesis Adviser

_____
Prof. Dr. Nikhil Koratkar, Member

_____
Prof. Dr. Theodorian Borca-Tasciuc, Member

Rensselaer Polytechnic Institute
Troy, New York

November, 2011
(For Graduation December 2011)

CONTENTS

LIST OF FIGURES

NOMENCLATURE

A	area of copper surface
a	constant used for correlation developed
a_d	constant used for dew point temperature calculation
b	constant used for correlation developed
b_d	constant used for dew point temperature calculation
c	constant used for correlation developed
c_1	constant
d	constant used for correlation developed
g	acceleration due to gravity
Gr_L	Grashof number for vertical flat plate
h	heat transfer coefficient
h_{cond}	heat transfer coefficient due to condensation
h_{evap}	heat transfer coefficient due to evaporation
h_{mp}	multiphase heat transfer coefficient
h_{sp}	single-phase heat transfer coefficient
k_{air}	thermal conductivity of air
k_{water}	thermal conductivity of water
L	characteristic length
Nu_{mp}	multiphase Nusselt number
Nu_{sp}	single-phase Nusselt number
Pr	Prandtl number
$\dot{Q}$	heat transfer rate
Ra_L	Rayleigh number for vertical flat plate
RH	relative humidity
T_1	surface temperature
T_2	temperature of thermocouple in block closest to surface
T_3	temperature of thermocouple in block farthest from surface
T_{amb}	ambient temperature
T_d	dew point temperature

α	thermal diffusivity
β	volumetric thermal expansion coefficient
$\gamma( )$	function used for dew point temperature calculation
ΔT	temperature difference between ambient and surface
ΔT_b	temperature difference within copper block
θ	non dimensional temperature variable
ν	kinematic viscosity

ACKNOWLEDGMENT

This thesis I undertook was a tremendous learning experience in more ways than one and along the way I have had the help and support of numerous people.

I would like to thank my advisor, Dr. Yoav Peles, for all his support and insight that guided me through this endeavor. His knowledge was instrumental in helping me grasp the important concepts that led to the thesis.

I would also like to thank the other members of my thesis defense committee, Dr. Nikhil Koratkar and Dr. Theodorian Borca-Tasciuc. I work closely with Dr. Koratkar, my doctoral advisor, and his encouragement is ever motivating. Dr. Theodorian Borca-Tasciuc was gracious to agree to be on my thesis defense committee and I am grateful to him.

I am grateful to Dr. Michael Jensen and Dr. Gregory Hampson who took courses on convection heat transfer and conduction heat transfer respectively which taught me the importance of understanding the physics behind the experiments. I would also like to thank Glenn Saunders at the Rensselaer Center for Automation Technologies and Systems (CATS) for all his help with the experimental setup.

I am thankful to all my past and current labmates for their help and time in various situations. I am especially thankful to Kayvan for his belief in my potential as a researcher. His words have often made me think ‘out of the box’ and I thoroughly enjoy hashing out ideas with him. I would be remiss if I did not mention all my friends that have wished me well especially Shambhavi who always challenges me to dream big.

Lastly and most importantly I would like to thank my family. Appa – thank you for teaching me the importance of the logical, rational approach and leading by example. Amma – thank you for being Appa’s perfect foil and showing me the importance of creativity to generate novel ideas. Chin – thanks for setting the bar so high, I will always look to you for inspiration. Chedathi – thanks for being so easy to talk to, I will always look to you for support.

ABSTRACT

Dehumidification heat transfer is associated with low values of heat transfer coefficient because of the presence of non condensable gas and the absence of saturated vapor in the ambient. Here we studied the heat transfer mechanisms during dehumidification on a vertical copper surface. Heat transfer coefficient at various humidity levels and ambient-surface temperature differences were obtained. A correlation was developed to relate the heat transfer coefficient, relative humidity, and ambient-surface temperature difference. Variations of about ~200% in heat transfer coefficient were observed between low and high humidity levels. It was also observed that the heat transfer coefficient is higher for filmwise condensation than dropwise condensation during dehumidification unlike for pure condensation.

1. Introduction and Historical Review

The condensation of moisture from humid air, termed dehumidification, is important in many heat transfer applications such as condensing heat exchangers [1], [2] and solar distillation devices for water desalination [3].

Nusselt [4] pioneered work and presented an analytical method to determine the heat transfer coefficient for condensation of pure vapor. His treatment was based on assumptions like constant fluid properties, no subcooling of the condensate, negligible momentum convective changes through the film, stationary pure vapor, no drag on the downward motion of the condensate and heat transfer through the liquid film by conduction only [5]. The most important assumptions being that the vapor was saturated and there was no non-condensable gas present.

Later studies improved the analytical model by removing some of the original assumptions. Condensation heat transfer in the presence of non-condensable gases significantly reduces heat transfer [6], [7]. The buildup of non-condensable gas near the condensate film lowers the diffusion of the vapor from the ambient to the condensate film and reduces the rate of mass and heat transfer. Thus, it is necessary to solve simultaneously the conservation equations of mass, momentum, and energy for both the condensate film and the vapor-gas boundary layer together with the conservation of species for the vapor-gas layer. At the interface of the vapor-gas boundary layer and the condensate film, a continuity condition of mass, momentum and energy has to be satisfied. When the content of non-condensable gas is significant as in air-steam mixture the condensation can be treated as dehumidification.

1.1 Background

Heat transfer during condensation or dehumidification involves an ambient-surface temperature difference, ΔT, across the ambient vapor and the condensing surface. While looking at dehumidification it is important to define relative humidity. Relative humidity (RH) is defined as the ratio of the partial pressure of water to the saturated

vapor pressure at a particular temperature [8]. The traditional definition of *RH* is to express it as a percentage but we will be treating it as a humidity ratio. This temperature difference, ΔT, is used to determine the heat transfer coefficient, *h*, using Newton's Law of Cooling.

$$h = \frac{\dot{Q}}{A\Delta T} \qquad 1$$

The schematic of the processes involved during dehumidification heat transfer is shown in Figure 1. Since the condensing surface is at a much lower temperature than the ambient, condensation will occur. During dehumidification, the ambient is not saturated vapor so there will be evaporation from this condensing surface.

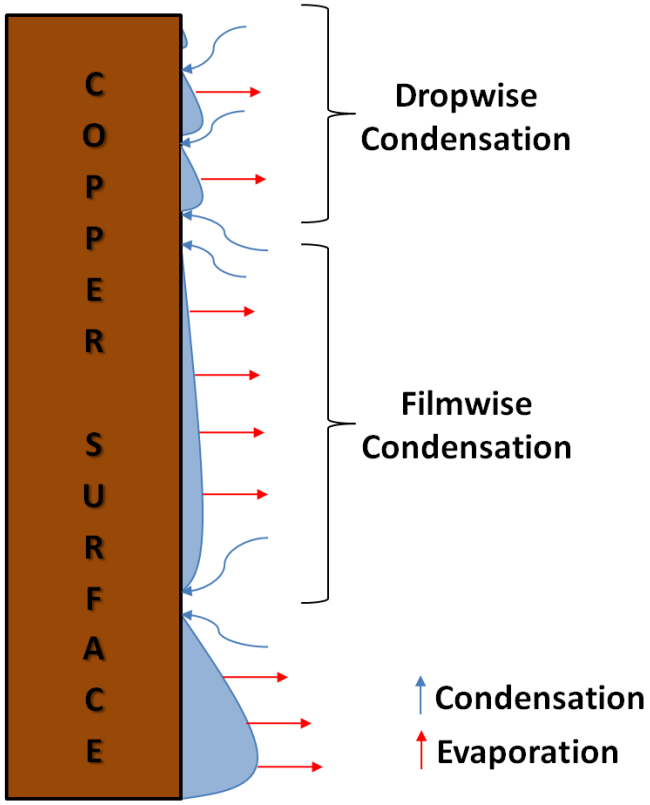

Figure 1: Schematic showing various processes that occur during dehumidification heat transfer.

The higher the ambient-surface temperature difference, ΔT, for the same heat transfer rate, $\dot{Q}$, the lower the heat transfer coefficient, *h*, is. This ambient-surface

temperature difference, ΔT, is shown as a schematic in Figure 2 and can be expressed as a sum of several components, [9]

$$\Delta T = T_{amb} - T_s = \Delta T_v + \Delta T_\delta + \Delta T_{cap} + \Delta T_{drop/film} \quad (2)$$

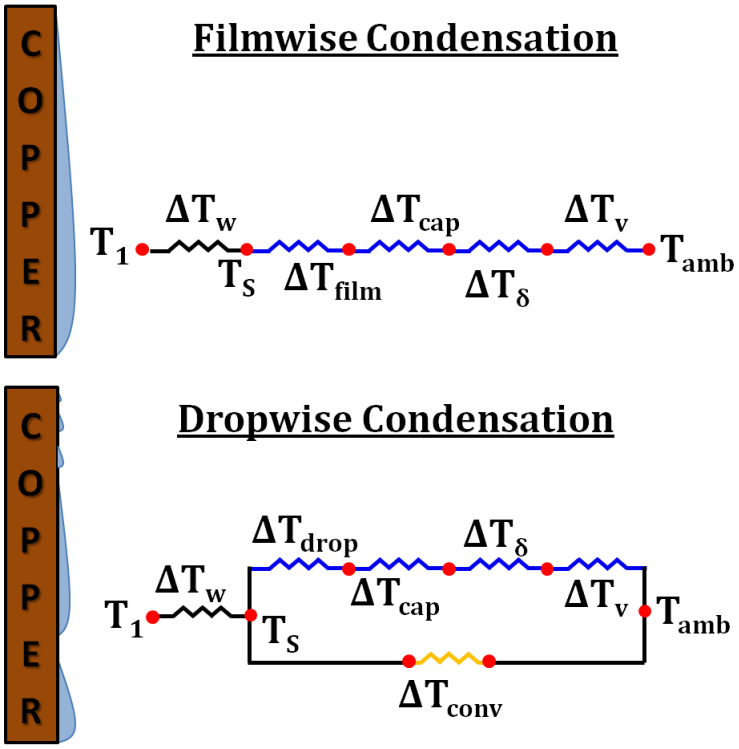

Figure 2: Schematic to show temperature drops due to different thermal resistances.

The temperature drop across the wall, ΔT_w, can be significant if the surface oxidizes or becomes contaminated thereby forming a region of increased thermal resistance. This is a factor if the temperature measurement made below the surface, and not on the surface, as in our experimental setup discussed in section titled *Materials and Apparatus*.

The temperature drop across the vapor, ΔT_v, for pure condensation is generally negligible. The thermal resistance in the vapor can be ignored because it is usually an order of magnitude less than the other thermal resistances. This low contribution to the overall resistance is the result of the ability of the vapor to mix extremely well for both

free and forced convection. Mixing allows enhanced heat and mass transfer towards the cooler surface. However, the thermal resistance of the vapor needs to be taken into account when dealing with condensation of vapor mixtures that include an inert gas (non-condensable gas). The inert gas effectively insulates the conduction of heat through the vapor. This is a very important factor in dehumidification and is the reason for much lower values of heat transfer coefficients, *h*, than in pure condensation of vapor.

The temperature drop due to the thermal resistance encountered at the vapor-liquid interface, ΔT_{δ}, is again negligible. This temperature drop has an analytical expression given by Faghri [10]. It is important to note that this thermal resistance is found in both dropwise and filmwise regimes and the expression to determine them are similar.

According to Graham & Griffith [11] there exists a temperature drop, ΔT_{cap}, due to the slight depression of the equilibrium interface temperature below that of the normal saturation temperature for a droplet of diameter D. This thermal resistance also exists for filmwise regime and is similar in magnitude.

The temperature drop due to conduction of heat through the droplets or film, $\Delta T_{drop/film}$, is usually the limiting thermal resistance for pure condensation [11]. This is because the largest temperature drop in the condensation process occurs in the film or droplet, even though the conduction path is relatively short in comparison to the other heat flow lengths in the condensation process. This leads to high thermal resistances and low heat transfer coefficients. Filmwise condensation has a higher temperature drop because of this thermal resistance component and hence lower heat transfer coefficient.
In summary the thermal resistance associated with vapor, interfacial resistance and capillary depression will be the same for both dropwise and filmwise condensation. The conduction resistances found in dropwise and filmwise condensation is different and hence the values of heat transfer coefficient, *h,* obtained is different.

1.2 Literature Review

Experimental [12] and modeling studies [1], [2] have shown that the heat transfer coefficient is lower for dehumidification than for pure condensation. This has been attributed to the thermal resistance of the boundary layer of moist air [6], [7].

The heat transfer during dehumidification of flowing air-water (humid air) mixture was experimentally investigated for a vertical plate. Yaghoubi et al. [13] developed a correlation for heat and mass transfer for laminar flow of humid air over a cooled plate with dehumidification for relative humidities above 50% and 40 ^{o}C $<T_{ambient}<$ 90 ^{o}C. The correlation, given in equation 3, was derived from numerical results and showed an increase in Nusselt number with increasing relative humidity. Yaghoubi et al. validated their correlation with experimental results of Legay-Desesquelles and Prunet-Foch [14] who looked at saturated air-steam flow.

$$Nu_{x,sen} = \frac{0.902Re^{0.5}\left(\left(P_{WV} - P_{sat}\right)/\left(P_{atm}\right)\right)^{0.337}\phi^{0.177}}{\left(P_{WV}/P_{atm}\right)^{0.337}} \quad (3)$$

For humid air the percentage of non condensable gas is in much higher quantities. Correlations looking at the effect of relative humidity over the entire range have not been developed for stationary humid air although practical applications exist.

Nagai et al. under took investigation of heat transfer characteristics for different orientations of condensation surface in humid air [3]. They report a linear relationship between heat transfer rate, $\dot{Q}$, and ambient-surface temperature difference, ΔT, indicating a constant heat transfer coefficient, h, for relative humidity values between 40 to 90% and ambient humid air temperatures of 50 – 70 ^{o}C. Nagai et al. reported heat transfer coefficients, h, of about 100 W/m^{2}K for an ambient-surface temperature difference , ΔT,

of 20 ^{o}C and chamber temperature, T_{amb}, of 60 ^{o}C with a relative humidity, RH, of 0.7 [3].

2. Research Objectives

We aim to experimentally study the heat transfer process during dehumidification for the entire range of *RH* values from 0.1 to 0.9. We will determine a correlation that relates heat transfer coefficient, *h*, and independent factors like ambient-surface temperature difference, ΔT, and relative humidity, *RH*. We will show through our experiments that in dehumidification the limiting thermal resistance is due to the noncondesable gas and/or wall thermal resistance because the values of heat transfer coefficient, *h*, do not drop significantly from dropwise regime to the filmwise regime. We also show that since these experiments are conducted at various values of relative humidity, *RH*, always less than unity, there will always be evaporation which reduces the heat transfer coefficient significantly.

3. Research Plan

Experiments to determine the heat transfer coefficient, *h*, were conducted such that each set of data, for a particular chamber temperature, T_{amb}, and relative humidity, *RH*, was obtained by controlling the temperature of the serpentine cooling channel. At a relative humidity, *RH*, of 1 the partial pressure of water is equal to the saturated vapor pressure and no net evaporation occurs. However, when the relative humidity, *RH*, is less than 1, there will always be some evaporation that occurs. Evaporation is inversely proportional to *RH* so the rate of evaporation is high at low *RH*.

Experiments began at low heat transfer rates, $\dot{Q}$, corresponding to convection regime in which no condensation occurred. The coolant flow was then controlled to lower the surface temperature, T_1, below the ambient temperature, T_{amb}, and the setup was allowed to reach steady state before the next value was recorded. The surface was visually monitored to determine when condensation occurred. This visual inspection proved to be misleading since an increase in heat transfer coefficient, *h*, was observed before apparent condensation was observed. All data points until the onset of condensation occurred were considered to be in the convection regime and all further data points were in the dehumidification regime.

To determine pure convection (single-phase) characteristics, the surface was heated with respected to the ambient. The value of heat transfer coefficient, *h*, under these conditions is the single-phase heat transfer coefficient, h_{sp}. The surface was then cooled until the surface temperature, T_1, dropped below the ambient temperature, T_{amb}, and this constituted the cooling convection regime. From single-phase to cooling convection the heat transfer coefficient, *h*, did not vary significantly. The point at which the single-phase heat transfer coefficient, h_{sp}, increased abruptly denoted the point at which dehumidification started and this was the multiphase heat transfer coefficient, h_{mp}.

4. Materials and Apparatus

Figure 3 depicts the experimental setup and its components. The setup involves controlling the temperature of a copper surface and varying it to fixed values above and below the ambient temperature, T_{amb}, in a chamber whose relative humidity, RH, is known and can be controlled.

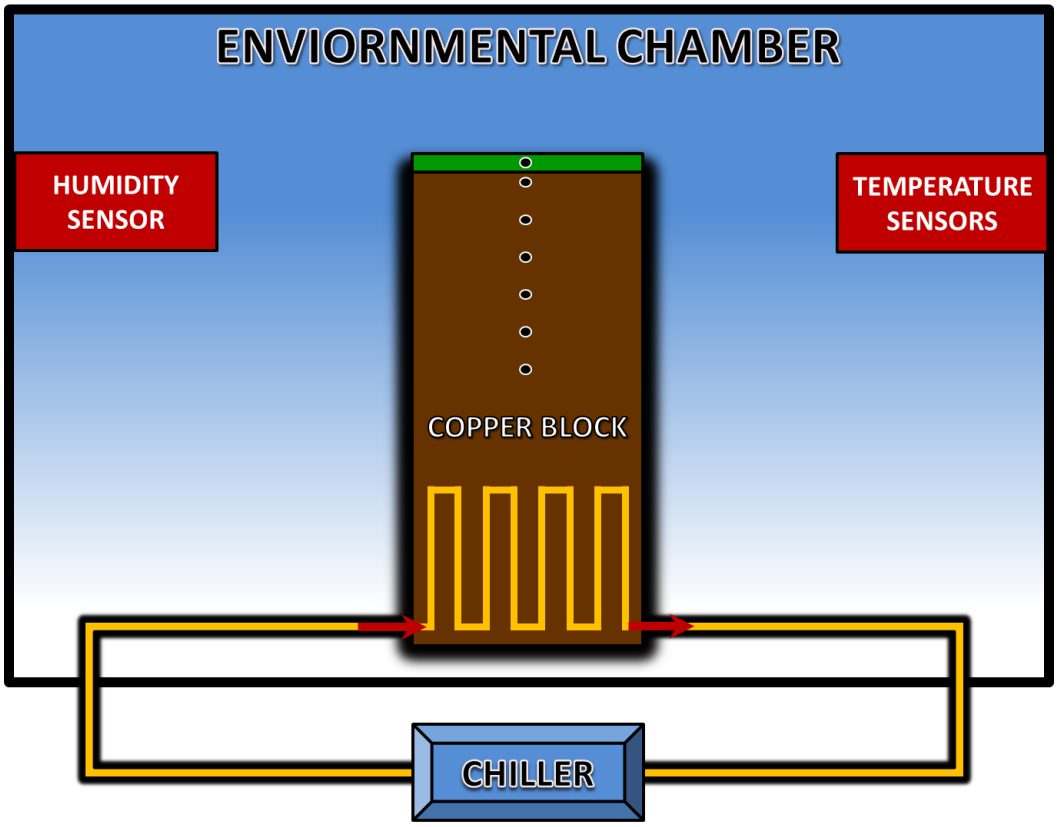

Figure 3: Schematic of the experimental setup

4.1 Copper Surface

Dehumidification was studied on the surface of copper disc, having a 39 mm diameter heat transfer area, as seen in Figure 4. The copper disc has a stepped contour to allow it to fit into the copper block. The copper surface and block was designed as two separate parts and not as a single integral component as it would allow for easy surface modifications to the surface rather than modifications to the entire block. Replacement of the copper block for every new surface to be tested would be impractical as it has a

complex design. Oxygen free copper was used for both the copper surface and copper block components because of its high thermal conductivity.

The copper surface has a cylindrical hole, 1 mm in diameter which is 19.5 mm deep and located 1.5 mm below its surface and runs parallel to it. This is for the introduction of a thermocouple which measures the surface temperature, T_1.

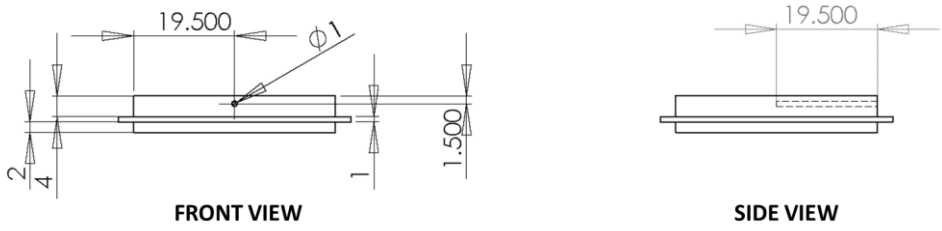

Figure 4: Front (left) and side (right) views of the copper surface. All dimensions shown are in mm.

This copper surface component fits into the copper block, shown in Figure 5, which is used to measure the heat transfer rate.

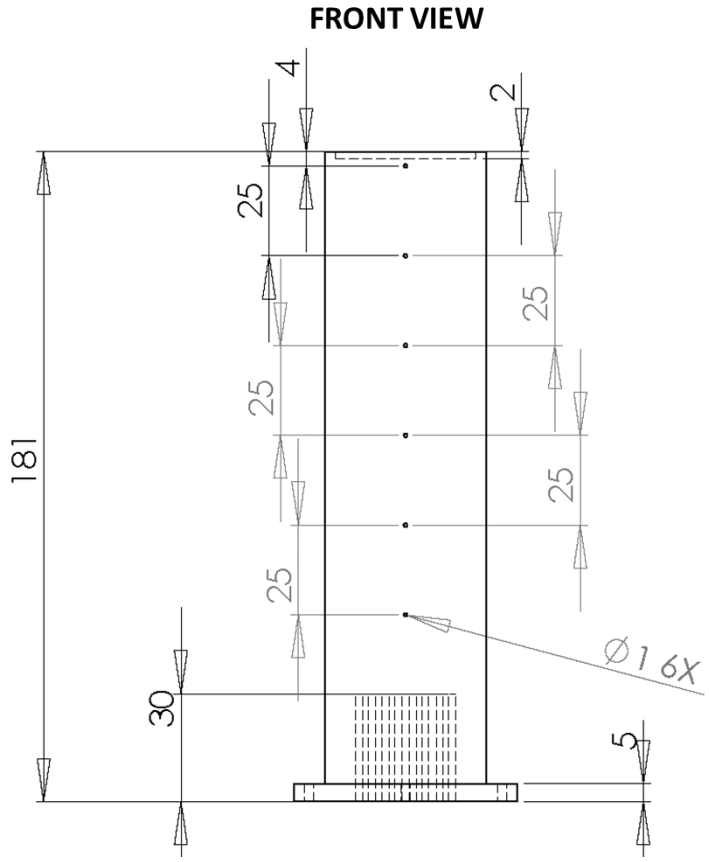

Figure 5: Cross sectional view of the copper block. All dimensions shown are in mm.

4.2 Copper Block

A copper block was designed to serve the dual purpose of measuring the heat transfer rate, $\dot{Q}$, through the copper surface with sufficient confidence and control the heat transfer rate, $\dot{Q}$. The first criterion was addressed by making 6 thermocouple slots, as seen in Figure 5, to measure the temperature along the block and calculate the heat transfer rate, $\dot{Q}$, using Fourier's Law of Heat Conduction. The second criterion was taken care of by designing a serpentine channel at the bottom of the block, shown in Figure 6, through which a temperature controlled heat transfer fluid was passed that controls the heat transfer rate, $\dot{Q}$, through the copper block.

The thermocouple slots are 1 mm diameter holes hat extend a length of 19.5 mm to the centre of the copper block. The first thermocouple (T_1) slot in the copper block is at a depth of 2 mm from the circular slot surface. The remaining 5 slots are at an equal distance of 25 mm each. The cooling fluid passes through a continuous serpentine channel as shown in Figure 6. The serpentine channel arrangement is used to maximize the cooling heat capacity of the block as condensation involves high heat transfer coefficients.

The copper block is insulated from the chamber by a cylindrical Delrin insulation with only slots for the thermocouple probes (Figure 7). This insulation component slides onto the copper block like a sleeve serving to push the copper surface down onto the copper block ensuring better contact and lower thermal thermal contact resistance. Additionally thermal paste, Ceramique 2 (ceramic based thermal paste) produced by Arctic Silver, is used to ensure good thermal contact. An additional air insulation layer between Delrin and copper block was also provided.

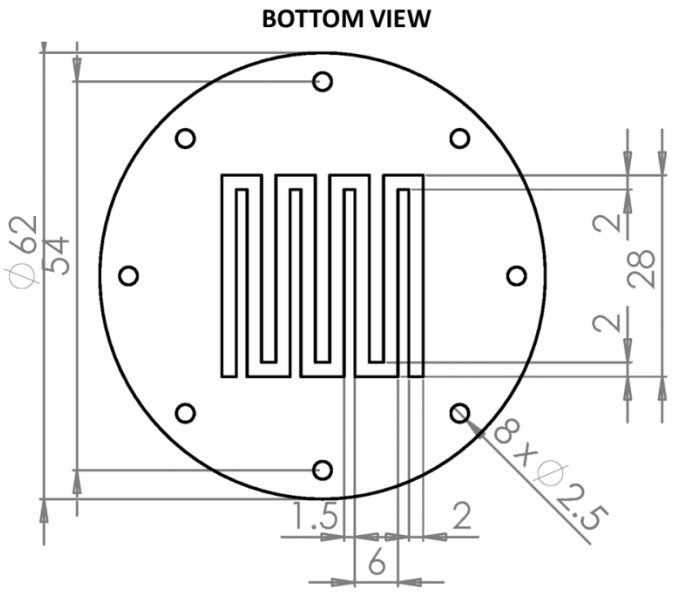

Figure 6: Bottom view of the copper block showing serpentine channel. All dimensions shown are in mm.

A base plate, made of Delrin, seals the serpentine channel at the bottom while simultaneously preventing the copper block from coming into contact with the hot chamber conditions. The base plate is provided with an O-ring seal to prevent any leak of heat transfer fluid. There are holes for 8 screw fasteners (Figure 6) that hold the copper block, Delrin insulation and base plate together. The insulation is provided to ensure that the heat flux is uniform and one-dimensional which simplifies calculation of the heat transfer coefficient, *h*. The copper surface along with the block, insulation and base plate are also shown in Figure 7.

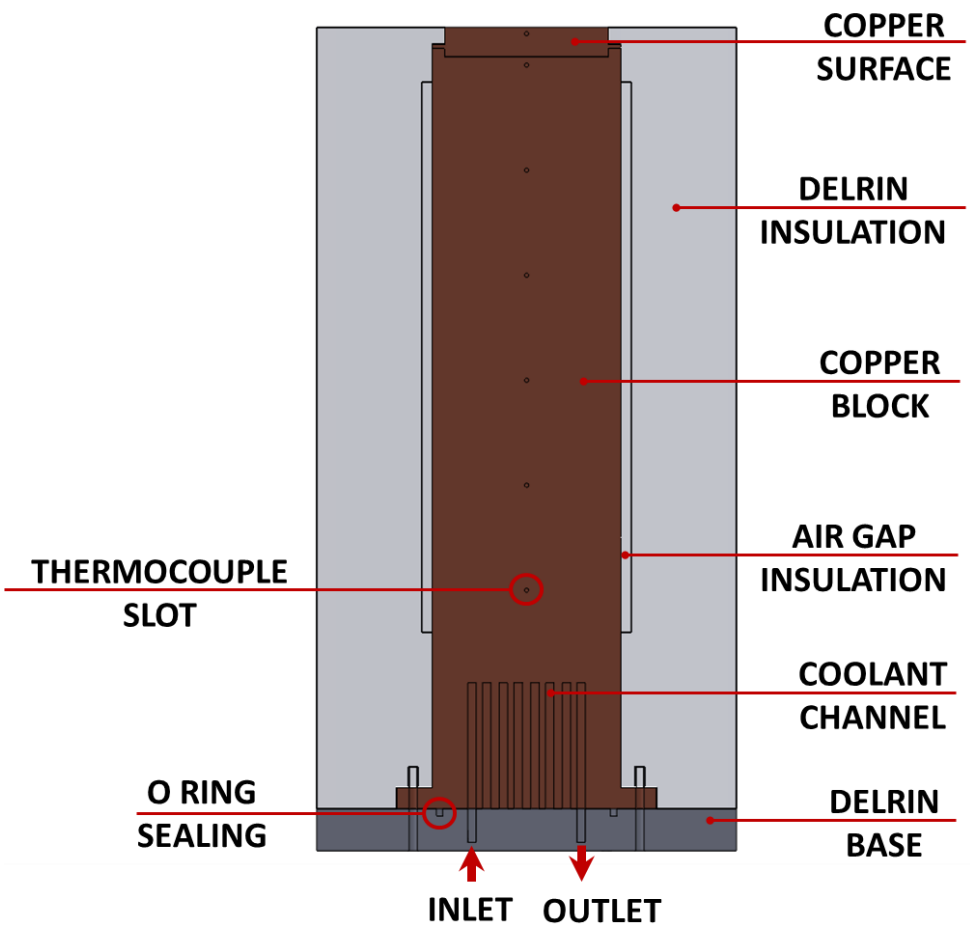

Figure 7: Cross-section of copper surface, block, insulation and base plate.

4.3 Environmental chamber

The equipment used to control the relative humidity, RH, of the environment that houses the dehumidification surface is a Thermotron SM-8 Environmental Test Chambers with a 3800 Programmer/Controller. The chamber has a workspace volume of 227 L, an ambient temperature, T_{amb}, range of – 68 ^{o}C to 180 ^{o}C and a relative humidity, RH, range from 0.1 to 0.98. The humidity sensor is a solid state high accuracy electronic sensor (+/- 0.5%).

4.4 Chiller

The equipment that provides heat transfer fluid in the external closed loop through the serpentine channels of the copper block was RC-6 Lauda-Brinkmann Low-

temperature thermostats. The chiller's bath liquid is Kryo 30 (recommended for the chiller) which has similar characteristics as ethylene glycol. The chiller was set at the maximum bath fluid flow rate and this remains constant for all measurements. The temperature of the bath was set to the desired value and was used to control the heat transfer rate through the block. The heat flux through the block was calculated using the high accuracy thermocouple system. External piping is insulated to minimize heat losses to/from the circulating fluid.

4.5 Temperature measurement

The temperature measurements were obtained using a high accuracy GEC Model S7TC precision thermocouple (T type) scanner with 7 input channels. National Institute of Standards and Technology (NIST) traceable instrument calibration together with the thermocouple system were used to achieve a measurement accuracy of ± 0.05 °C or better over a temperature range of 0 to 140 °C with a resolution of 0.01 °C. One channel was used to obtain accurate readings of the ambient temperature, T_{amb}, near the dehumidification surface. One channel is used to determine the surface temperature, T_1, of the copper disc using slot (T_1) while another two channels are used to measure the maximum (T_2) and minimum temperature (T_3) of the block. The remaining two channels are used in alternate slots along the copper block to ensure constant heat flux.

4.6 Summary of setup

Below is a summarized description of each component and its role in the experimental setup.

1. Copper surface: This is the component on which dehumidification is studied.
    a. Copper block – Required to measure the heat transfer rate, $\dot{Q}$, to the copper surface for multiple surfaces.
    b. Insulation – Ensures one-dimensional heat transfer.
2. Environmental Chamber: Required to control ambient temperature, T_{amb}, and relative humidity, *RH*, accurately.

3. Chiller: Required to control the copper surface temperature by circulating a heat transfer fluid continuously while maintaining its temperature at a predetermined level.
4. Temperature sensors: Required to measure the ambient temperature, T_{amb}, surface temperature, T_1, and block temperature, T_2 and T_3. These temperature measurements are used to calculate the parameters of interest.

5. Discussion and Conclusions

The experimental values obtained from the thermocouple system are ambient temperature, T_{amb}, surface temperature, T_1, and internal block temperature difference, ΔT_b. From here onwards the surface-ambient temperature difference will be referred to as ΔT, and internal block temperature difference as ΔT_b.

$$\Delta T = T_{amb} - T_1 \quad (4)$$

$$\Delta T_b = T_2 - T_3 \quad (5)$$

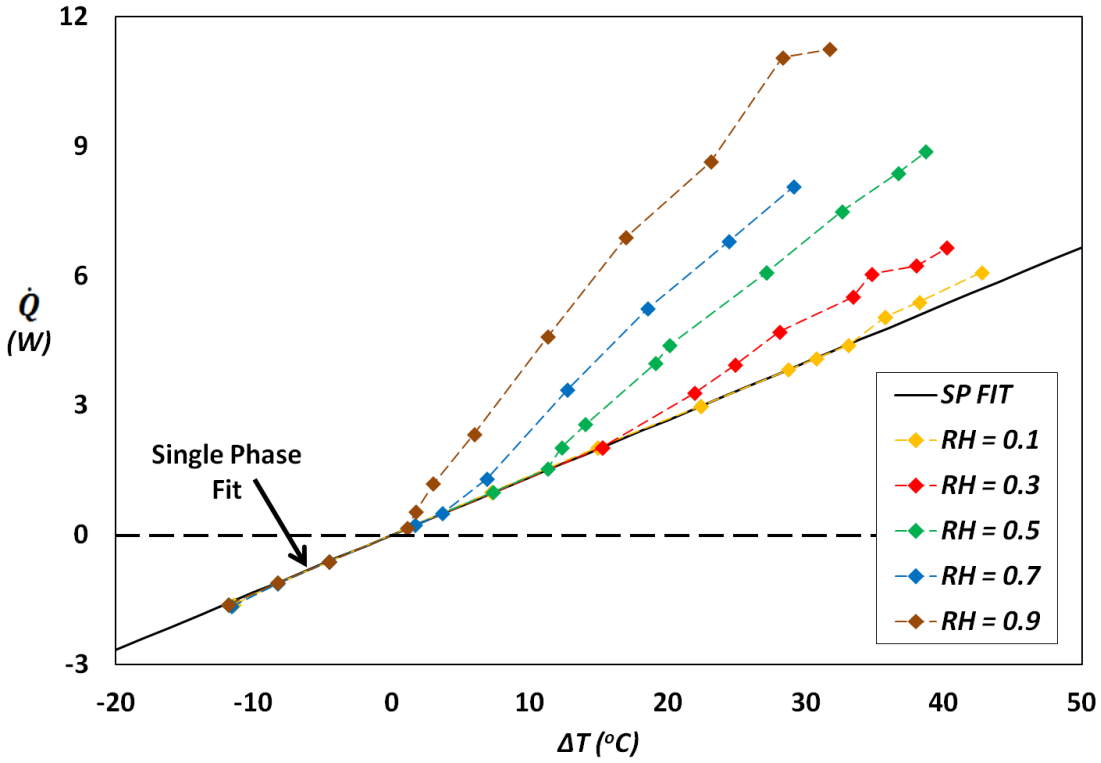

Figure 8: Heat transfer rate ($\dot{Q}$) as a function of ambient-surface temperature difference (ΔT) for various relative humidities, RH.

The heat transfer rate through the block, $\dot{Q}$, is shown in Figure 8 and is calculated from the internal block temperature difference, ΔT_b, as follows:

$$\dot{Q} = \frac{kA\Delta T_{\mathrm{b}}}{L} \quad \textbf{6}$$

When the surface is heated with respect to the ambient, i.e., surface-ambient temperature difference, *ΔT*, is less than zero, heat is transferred through single-phase convection. During single-phase convection, all points below the dashed line in Figure 8 , all curves corresponding to different relative humidity values are identical. The heat transfer coefficient, h, can be calculated as,

$$\dot{Q} = hA\Delta T \quad \textbf{7}$$

The heat transfer surface area, *A*, is constant. The only parameter that controls the relation between heat transfer rate, $\dot{Q}$, and ambient-surface temperature difference, *ΔT*, is the heat transfer coefficient, *h*. Also the heat transfer coefficient, *h*, determines the slope of the curve when heat transfer rate, $\dot{Q}$, is plotted as a function of surface-ambient temperature difference, *ΔT*, and this slope will remain constant as long as the heat transfer coefficient, *h*, is constant.

Hence in Figure 8, as discussed before, the slope of the plots for all relative humidity values are constant and these points are fitted to a linear function. The value of the single-phase heat transfer coefficient, h_{sp}, is obtained,

$$\dot{Q} = c_1\Delta T, \quad c_1 = 0.1332 \text{ W/K}$$

$$h_{sp} = \frac{c_1}{A}, \quad h_{sp} = 111.5 \text{ W/m}^2\text{K}$$

The black solid line in Figure 8 is the line corresponding to single-phase heat transfer and any point outside this line corresponds to partial or full condensation associated with increased heat transfer coefficients, *h*.

Figure 8 also shows that the heat losses from the system are negligible; the assumption of 1-D heat conduction through the block is a valid assumption, and that the system built is reliable to perform dehumidification experiments.

Since single-phase heat transfer coefficient, h_{sp}, does not change with relative humidity, *RH*, the chamber conditions are exactly the same for all humidities in terms of induced humid air flow patterns. This is important because it allows making assumptions later that no additional forced convection component is active at higher humidities.

For natural convection heat transfer shown below is the range of the values expected for the non dimensional Grashof number, Gr_L, and Rayleigh number, Ra_L [15],

$$Gr_L = \frac{g\beta(T_{amb} - T_1)L^3}{v^2} \cong 2 \times 10^4 - 7.5 \times 10^4 \quad \textbf{8}$$

$$Ra_L = Gr_L Pr = \frac{g\beta(T_{amb} - T_1)L^3}{v\alpha} \cong 1 \times 10^4 - 5.5 \times 10^4 \quad \textbf{9}$$

Since the Rayleigh number is much less than 10^9, the free convection flow is laminar in the current experiments [15]. Using the correlation developed for laminar natural convection [15], the expected values of average Nusselt number (Nu_{sp}) and average heat transfer coefficient (h_{sp}) values are estimated below,

$$g(Pr) = \frac{0.75Pr^{1/2}}{(0.609 + 1.221Pr^{1/2} + 1.238Pr)^{1/4}} \quad \textbf{10}$$

$$Nu_{sp} = \frac{h_{sp}L}{k_{air}} = \frac{4}{3}\left(\frac{Gr_L}{4}\right)^{1/4} g(Pr) \cong 5.9 - 7.7 \quad \textbf{11}$$

$$h_{sp} = \frac{Nu_{sp}k_{air}}{L} \cong 4.3 - 5.7\ W/m^2K \quad \textbf{12}$$

The experimental values of single-phase heat transfer coefficient, h_{sp}, are higher at around 111.5 W/m^{2}K and this could be attributed to the air flow inside the chamber due to its construction to allow for addition of humid air to change the relative humidity, *RH*, when required. However, it is important to note that this existing humid air flow in the chamber is the same for all humidity conditions and plays no additional role as evidenced by the fact that the single-phase heat transfer coefficient, h_{sp}, is same for all humidity values.

Another observation that provides insight into dehumidification heat transfer is that the point of deviation of the curves from the single-phase fit for various values of relative humidity, *RH*, is different. As seen in Figure 8 the curve for the highest relative humidity, *RH* = 0.9, deviates from the single-phase curve at a very low positive value of ΔT and as the relative humidity, *RH*, decreases the point of deviation from the single-phase fit increases. At high relative humidity a very small surface-ambient temperature difference, ΔT, is sufficient to initiate condensation but at low humidity it takes a very high surface-ambient temperature difference, ΔT, to initiate condensation. This suggests that the surface temperature is also important with varying values of relative humidity.

5.1 Dew point and use of *Nu*

First the dew point, T_d, needs to be determined as the temperature to which air must be cooled in order to reach saturation (assuming air pressure and moisture content are constant). A higher dew point, T_d, indicates more moisture present in the air [16].

For various values of relative humidity, *RH*, the dew point temperature, T_d, can be calculated using the following relations [17],

$$T_d = \frac{b_d \gamma(T_{amb}, RH)}{a_d - \gamma(T_{amb}, RH)} \quad \textbf{13}$$

$$\gamma(T_{amb}, RH) = \frac{a_d T_{amb}}{b_d + T_{amb}} + \ln(RH) \quad \begin{matrix} a_d = 17.271 \\ b_d = 237.7\ ^oC \end{matrix} \quad \textbf{14}$$

Ideally when the surface temperature, T_1, reaches the dew point, T_d, condensation of the water from the humid air begins. However, it is observed that condensation begins even when the surface temperature is slightly higher than the theoretical dew point. It is, therefore, convenient to define the following non-dimensional parameter, θ,

$$\theta = \frac{T_d - T_1}{T_{amb} - T_1} \quad \textbf{15}$$

Note that in the above relation the denominator ($T_{amb} - T_1$) is always positive so when θ is negative it implies that the surface temperature, T_1, is higher than the dew point, T_d.

Figure 9 depicts the condensation multiphase Nusselt number, Nu_{mp}, as a function of the non-dimensional temperature ratio, θ, for various surface temperatures. The multiphase Nusselt number, Nu_{mp}, differs from the single-phase Nusselt number, Nu_{mp}, since they are defined using different values of fluid thermal conductivity for normalization. Shown below are the exact relations used,

$$Nu_{sp} = \frac{h_{sp}L}{k_{air}} \; ; \quad Nu_{mp} = \frac{h_{mp}L}{k_{water}} \; ; \quad \textbf{16}$$

This is done to maintain consistency with the definition of Nusselt number as the ratio of convective to conductive heat transfer across the boundary. For the case of single-phase heat transfer the fluid at the boundary is humid air while during multiphase heat transfer the fluid is water.

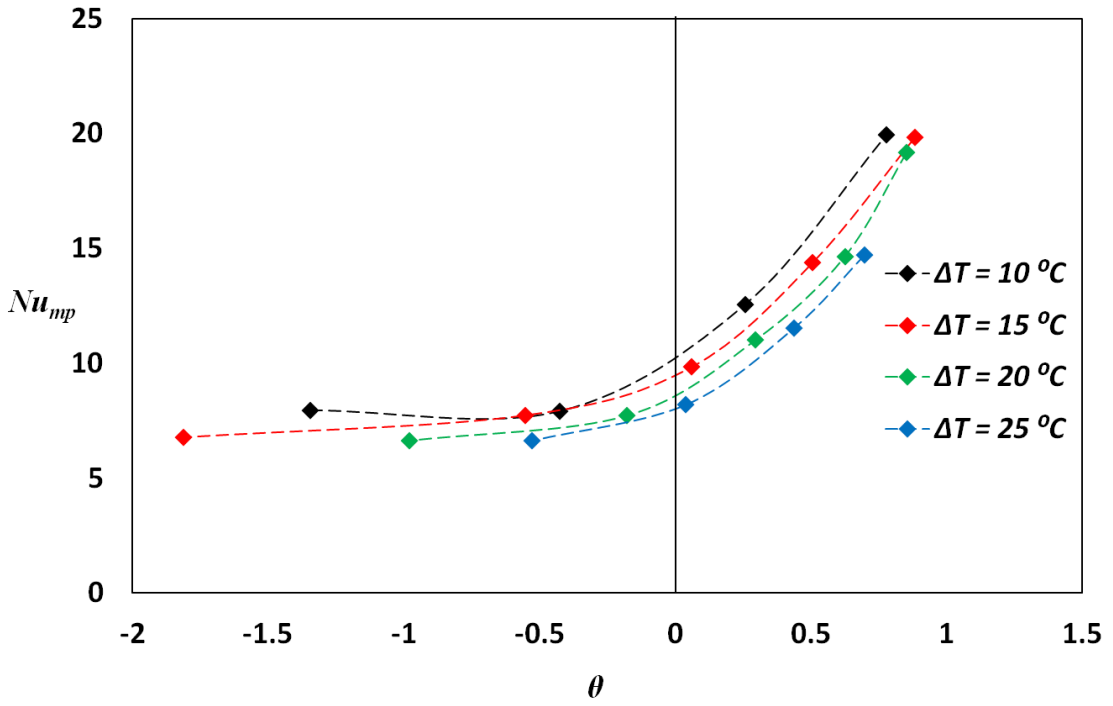

Figure 9: Multiphase Nusselt number (Nu_{mp}) as a function of the non-dimensional temperature ratio (θ) for various heat flow values is shown.

From Figure 9 it can be seen that while the surface temperature, T_1, is higher than the dew point, T_d, (θ is negative) the change in the multiphase Nusselt number, Nu_{mp}, and consequently multiphase heat transfer coefficient, h_{mp}, is very minor, and corresponds to dropwise condensation as observed visually. However, when the surface temperature, T_1, is lower than the dew point, T_d, (θ is positive) there is a dramatic increase in multiphase Nusselt number, Nu_{mp}, for small increments of θ. It follows that for humid air, when the surface temperature, T_1, is below the dew point, T_d, dropwise condensation is initiated but this does not significantly enhance heat transfer. However as dropwise condensation transitions to filmwise condensation the heat transfer coefficient, h_{mp}, increases. This is unlike the case for pure vapor condensation where dropwise condensation has significantly higher heat transfer coefficients than filmwise regime.

5.2 Correlation for h_{mp}

Since multiphase heat transfer coefficient, h_{mp}, depends on the relative humidity, *RH*, and the surface-ambient temperature difference, ΔT, a correlation relating these terms can be developed. The relative humidity, *RH*, and surface-ambient temperature difference, ΔT, are selected as independent variables and multiphase heat transfer coefficient, h_{mp}, as the dependent variable. Power law dependence for relative humidity, RH, and surface-ambient temperature difference, ΔT, can be written according to,

$$h_{mp} = a + b(RH)^c(\Delta T)^d \quad \textbf{17}$$

Where *a*, *b*, *c* and *d* are constants.

Curve fitting with two independent variables was used to determine the constants *a*, *b*, *c* and *d* using commercial software DataFit version 9.0.59 developed by Oakdale Engineering. The curve fitting was carried out using 23 points that included values of relative humidity, *RH*, between 0.1 and 0.9 and values for surface-ambient temperature difference, ΔT, between 7 ^{o}C and 45 ^{o}C. The coefficients were found to fit the experimental results as shown below in equation 18,

$$h_{mp} = a + bRH^c\Delta T^d \qquad \begin{gathered} \boldsymbol{a = 110.96\ W/m^2K} \\ \boldsymbol{b = 203.11\ W/m^2K^{1.1}} \\ \boldsymbol{c = 2.17} \\ \boldsymbol{d = 0.10} \end{gathered} \quad \textbf{18}$$

The 'goodness of fit' or R^2 value is 0.965 which indicates a good fit. When the relative humidity, *RH*, is zero the multiphase heat transfer coefficient, h_{mp}, is about 110.96 W/m^{2}K and is almost equal to the single-phase heat transfer coefficient, h_{sp}. This is expected since for at a relative humidity, *RH*, of zero no condensation would occur.

Nagai et al. reported heat transfer coefficients, *h*, of around 100 W/m^{2}K for a surface-ambient temperature difference, ΔT, of 20 ^{o}C in an ambient temperature, T_{amb}, of 60 ^{o}C at a relative humidity, *RH*, of 0.7 [3]. This value of heat transfer coefficient, *h*, is

significantly lower than our value, which is around 220 W/m^{2}K, at similar conditions. If we subtract the single phase heat transfer coefficient, h_{sp}, component, due to mixed convection, we get a more realistic value of around 110 W/m^{2}K which is similar to the values obtained by Nagai et al. [3].

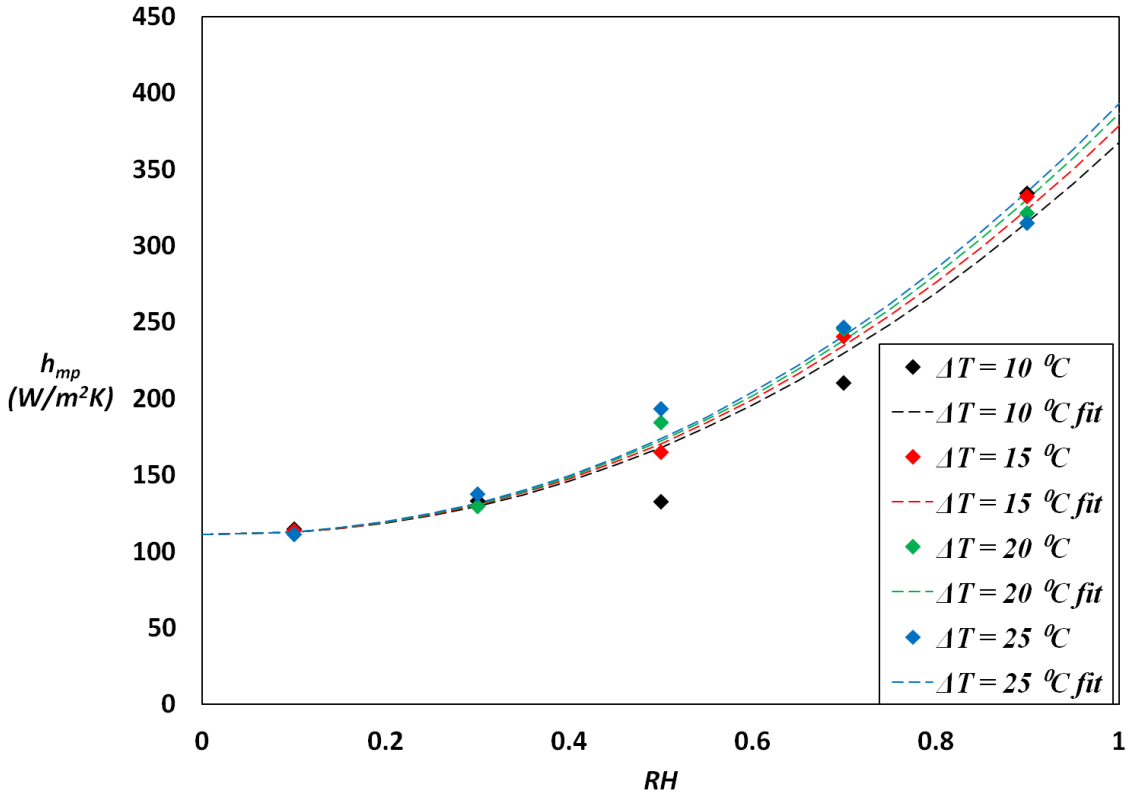

Figure 10: Multiphase heat transfer coefficient (h_{mp}) as function of relative humidity (*RH*) for various ambient-surface temperature differences (ΔT).

In Figure 10, a plot of multiphase heat transfer coefficient, h_{mp}, as function of relative humidity, *RH*, for various ambient-surface temperature differences, ΔT, is shown. The experimental values are plotted as explicit points and the correlation developed earlier, in equation 18, is plotted as dashed lines. As can be seen the agreement is very good except for the relative humidity value of 0.5. The dependence of the multiphase heat transfer coefficient, h_{mp}, on surface-ambient temperature difference, ΔT, is weak. The dependence of multiphase heat transfer coefficient, h_{mp}, on relative

humidity *RH* is significant and hence rapidly increases at higher humidity values. This is due to the increased rate of condensate formation at higher humidity values.

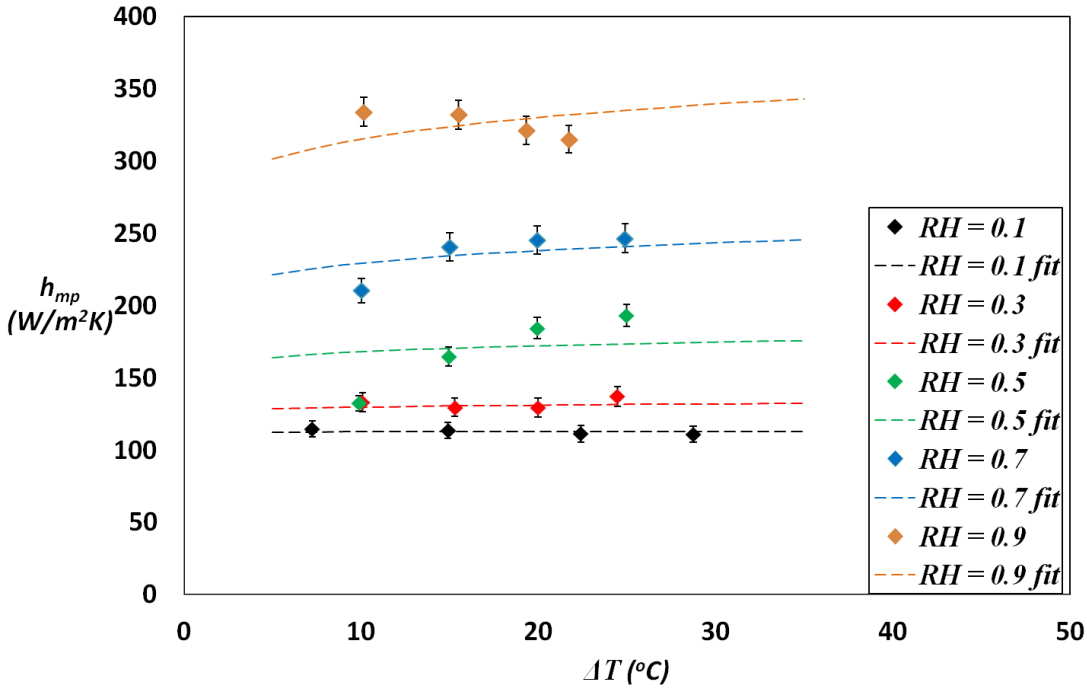

Figure 11: Multiphase heat transfer coefficient (h_{mp}) as function of ambient-surface temperature differences (ΔT) for various relative humidity (RH).

In Figure 11, the multiphase heat transfer coefficient, h_{mp}, is plotted as function of ambient-surface temperature difference, ΔT, for various values of relative humidity, RH. The experimental values are plotted as explicit points and the correlation developed earlier, in equation 18, is plotted as dashed lines.

An interesting point to note is that the correlation predicts an initial rapid rise in the multiphase heat transfer coefficient, h_{mp}, followed by a slow down. This could be due to the formation of a condensate film thick enough to inhibit heat transfer. This can be confirmed by the use of a super-hydrophobic layer, which does not allow condensate film formation rather maintains a dropwise regime. The difficulty would arise in choosing a suitable superhydrophobic layer that its thermal resistance does not reduce the heat transfer while promoting dropwise regime of condensate formation during

dehumidification. The liquid layer thermal resistance contribution to reduction in heat transfer is clearly seen at the highest relative humidity value of 0.9. The increasing condensate film forms sufficiently thick liquid layer that inhibits heat transfer and the heat transfer coefficient begin to drop.

The formation of a continuous condensate layer on the heat transfer surface that inhibits heat transfer explains the stagnating values of multiphase heat transfer coefficient, h_{mp}, after a certain limit. Evaporation is inversely proportional to the relative humidity, *RH*, so the rate of evaporation at low values of relative humidity, *RH*, will be high. Hence, this limit is not the same for all values of relative humidity, *RH*, but is a direct consequence of the humidity itself.

In our humid air system the maximum relative humidity, *RH*, used is 0.9 so there is always evaporation that occurs. In humid air systems, therefore, there is a balance between the phase-change processes of condensation and evaporation, which determines the overall multiphase heat transfer coefficient, h_{mp}.

Condensation involves cooling vapor to form a droplet by transferring the latent heat required for phase change to the copper block. Evaporation, on the other hand, transfers heat in the opposite direction to increase the latent heat of the droplet on the copper surface to convert it into vapor. Thus, the contribution to multiphase heat transfer coefficient, h_{mp}, by condensation, referred to here as, h_{cond}, will be opposite in sign to the contribution by evaporation, referred to here as, h_{evap}. The contribution of single-phase heat transfer coefficient, h_{sp}, and heat transfer coefficient due to condensation, h_{cond}, will be of the same sign since in both cases the fluid is cooled by the copper surface.

$$\boldsymbol{h_{mp} = h_{sp} + h_{cond} - h_{evap}} \qquad \textbf{19}$$

For the lowest relative humidity, *RH*, value of 0.1, evaporation dominates condensation and there is only a 7% increase of multiphase heat transfer coefficient, h_{mp},

over the single-phase heat transfer coefficient, h_{sp}. The enhanced evaporation explains the lack of significant increase in h_{mp} even though visual evidence of condensate formation (both filmwise and dropwise regimes) is observed. However, at high relative humidity, *RH*, values of 0.9 the condensation is vigorous while evaporation is minimal and hence a 200% increase in multiphase heat transfer coefficient, h_{mp}, is observed.

6. Summary

Considerable effort has been undertaken by the heat transfer community to extend knowledge about pure condensation and the effect of non-condensable gas. There have also been both experimental and computational studies to determine the heat transfer coefficient for humid air. However, the effect of relative humidity has not been looked at closely. In this work, an experimental setup to measure the heat transfer characteristics during dehumidification of humid air over copper surface was constructed. A correlation relating heat transfer coefficient, h, relative humidity, RH, and ambient-surface temperature difference, ΔT, was developed. Relative humidity, RH, was chosen as an independent variable because the aim was to study its effect on heat transfer characteristics. The ambient-surface temperature difference, ΔT was chosen as the second independent variable because it drives the convection and condensation processes.

The correlation developed satisfied all datum points with a good confidence level. It predicts the heat transfer coefficient, h, for all values of relative humidity, RH, including the limiting case of single-phase convection heat transfer.

The data suggests that relative humidity, RH, has a significant effect on the values of heat transfer coefficient, h. Large variations of heat transfer coefficient from ~ 113 W/m^2K at low relative humidity to ~ 330 W/m^2K at high relative humidity are observed. This ~200% increase in heat transfer coefficient is because the rate of evaporation at low humidity is very high and vice versa. Since the direction of heat transfer during evaporation and condensation are opposite, the rate of evaporation plays an important role during dehumidification heat transfer. During pure condensation heat transfer, the ambient is saturated with vapor so the effect of evaporation is negligible and hence the values of heat transfer coefficient are also much larger.

It was observed, during the data acquisition, that the heat transfer coefficient was lower during dropwise condensation than during filmwise condensation. This is unlike pure condensation heat transfer and can be explained by the presence of non condensable

gas which lowers the heat transfer coefficient. For pure condensation the vapor mixes freely which enhances heat and mass transfer to and from the droplet. During dehumidification, however, the non condensable gas forms an insulating layer that forms an additional thermal resistance that insulates the droplet from the vapor.

It was also observed that the original copper surface was oxidized and this reduces the heat transfer coefficient, *h*, as the oxide layer has a low thermal conductivity. The effect of this oxide can only be checked by passivating the surface with a suitably thin material.

7.

8. References

[1] A. M. Jacobi and V. W. Goldschmidt, "Low Reynolds Number Heat and Mass Transfer Measurements of an Overall Counterflow, Baffled, Finned-Tube, Condensing Heat Exchanger," *Int.l J. Heat Mass Transfer,* vol. 33, pp. 755-765, Apr. 1990.

[2] V. Srinivasan and R. K. Shah, "Condensation in Compact Heat Exchangers," *J. Enhanced Heat Transfer*, vol. 4, pp. 237-256, 1997.

[3] N. Nagai, M. Takeuchi, O. Kura, and T. Masuda, "Experimental Study on Free-Convection Condensation Heat Transfer from Moist Air," in *ASME Conf. Proc.*, San Francisco, 2005, pp. 305-309.

[4] W. Nusselt, "Die Oberflächenkondensation des Wasserdampfes," *Z. Vereins deutscher Ininuere*, pp. 541-575, 1916.

[5] J. G. Collier, *Convective Boiling and Condensation*. London: McGraw-Hill, 1981.

[6] W. J. Minkowycz and E. M. Sparrow, "Condensation Heat Transfer in the Presence of Noncondensables,Interfacial Resistance, Superheating, Variable Properties and Diffusion," *Int. J. Heat Mass Transfer,* vol. 9, pp. 1125-1144, Oct. 1966.

[7] E. M. Sparrow, W. J. Minkowycz, and M. Saddy, "Forced Convection Condensation in the Presence of Non Condensable Gas and Interfacial Resistance," *Int. J. Heat Mass Transfer*, pp. 1829-1845, Dec. 1967.

[8] R. H. Perry and D. W. Green, *Perry's Chemical Engineers' Handbook*, 7th ed. New York: McGraw-Hill, 1997.

[9] Global Digital Central. (2010, July) Thermal-Fluids Central. [Online]. Available: https://www.thermalfluidscentral.org. [Date Last Accessed, 11/08/2011].

[10] A. Faghri, *Heat Pipe Science & Technology*. Washington, D. C.: Taylor & Francis, 1995.

[11] C. Graham and P. Griffith, "Drop Size Distribution and Heat Transfer in Dropwise Condensation," *Int. J. Heat Mass Transfer*, pp. 337-346, Feb. 1973.

[12] M. Haji and L. C. Chow, "Experimental Measurement of Water Evaporation Rates into Air and Superheated Steam," *J. Heat Transfer*, vol. 110, pp. 237-242, Feb. 1988.

[13] M. A. Yaghoubi, H. Kazminejad, and A. Farshidiyanfar, "Heat and Mass Transfer with Dehumidification in Laminar Boundary Layer Flow Along a Cooled Flat Plate," *J. Heat Transfer*, vol. 115, pp. 785-788, Aug. 1993.

[14] F. Legay-Desesquelles and B. Prunet-Foch, "Heat and Mass Transfer with Condensation in Laminar and Turbulent Boundary Layers Along a Flat Plate," *Int. J. Heat Mass Transfer*, vol. 29, pp. 95-105, Jan. 1986.

[15] F. P. Incropera and D. P. Dewitt, "Free convecetion," in *Fundamentals of Heat and Mass Transfer*. New York: John Wiley & Sons, 2001, pp. 540-543.

[16] NWS Internet Services Team. (2009, June) National Oceanic and Atmospheric Administration. [Online]. Available: http://weather.gov/glossary. [Date Last Accessed, 11/08/2011].

[17] Paroscientific Inc. (2007, November) Paroscientific Inc. [Online]. Available: http://www.paroscientific.com/dewpoint.htm. [Date Last Accessed, 11/08/2011].